Journal of Chromatography A, 1289 (2013) 80–87

Contents lists available at SciVerse ScienceDirect

Journal of Chromatography A

journal homepage: www.elsevier.com/locate/chroma

Design and implementation of injector/distributor structures for microfabricated non-porous pillar columns for capillary electrochromatography

Sertan Sukas[a,*], Gert Desmet[b], Han J.G.E. Gardeniers[a]

[a] Mesoscale Chemical Systems, MESA+Institute for Nanotechnology, University of Twente, PO Box 217, 7500AE Enschede, The Netherlands
[b] Department of Chemical Engineering, Vrije Universiteit Brussels, Pleinlaan 2, 1050 Brussels, Belgium

ARTICLE INFO

Article history:
Received 29 November 2012
Received in revised form 6 March 2013
Accepted 9 March 2013
Available online 21 March 2013

Keywords:
Capillary electrochromatography
Microchip electrochromatography
Microfabricated columns
Microchannel injector
Flow distributor
Pillar columns

ABSTRACT

A previously proposed foil definition is applied in the design of injector/distributor structures for solid microfabricated column structures for capillary electrochromatography. In addition to a typical bifurcated distributor, an optimized design alternative with two different configurations is experimentally evaluated. Optimized designs yielded a flat profile for the injected sample with a maximum of 3% variation from the mean width, while it went up to 18% for the typical bifurcated distributor. The implemented electrokinetic injection approach enabled controlling the volume of the injected sample accurately without sacrificing the compactness of the device design. The width of the injected sample was directly proportional to the injection time, namely 165 and 218 μm base widths were obtained for 0.6 and 0.8 s of feeding, respectively. Reducing the external porosity of the distributor by 85% compared to the typical design, optimized distributors caused a decrease in the mean flow velocity of up to 70%. However, having a flat initial plug shape enabled the separation of a mixture of Coumarin 440, 460, 480 and 540 at 1 mm downstream of the injection point in 80 s, while it was even not possible to detect the C440 signal for a typical bifurcated design.

1. Introduction

When Regnier and his co-workers introduced the idea of microfabricated column structures for capillary electrochromatography (CEC) in 1998, they also proposed a "collocated monolithic collector" as a distributor/collector design for their "collocated monolithic support structures" (COMOSS) [1]. The coupling channel was divided into two equally wide and deep channels at every branching step until the created channel network fitted the desired column geometry. The aim was to enable uniform distribution and collection of analytes by keeping the total lateral cross-sectional area of the channels constant along the channel. It was stated that this kind of architecture also avoided solvent degassing. Several follow-up studies have since been published focusing on the effect of the geometries of support structures on performance [2,3], substrate materials [4] and in-line optical detection [5]. In all these studies the original distributor/collector design was preserved. Since keeping the total cross-sectional area constant was only possible by implementing hexagonal structures for channel branching, similar shapes (hexagon and diamond) were preferred as column geometries for easy interfacing of the collector/distributor with the column. Therefore, the effect of the injected plug shape on the separation performance was not investigated.

Desmet's group published a series of theoretical and experimental papers in the field of HPLC, reporting various designs for injectors for interfacing the conventional injection/detection systems to microchips and collectors/distributors which replace the turning geometries needed to increase the length of the channels for higher separation performance [6–8].

We recently published a theoretical study in the field of CEC on the optimization of the shape and positioning of the microfabricated solid pillars as column structures [9]. A new geometry, a foil definition, was introduced to replace the basic geometrical shapes used by others. It was experimentally validated that the performance of the microfabricated column structures can be maximized by the newly proposed foil definition [10]. In that study a bifurcated injector design similar to the ones reported earlier in literature was implemented. The aim of the present study is to extend the previous work by applying the validated foil-based design methodology to injector/distributor structures. These structures will be optimized in order to delimit injected sample plug dispersion, while keeping the possibility to control the injected sample volume for CEC.

* Corresponding author. Tel.: +31 053 4892604; fax: +31 053 4893595.
E-mail address: s.sukas@utwente.nl (S. Sukas).

0021-9673/$ – see front matter © 2013 Elsevier B.V. All rights reserved.
http://dx.doi.org/10.1016/j.chroma.2013.03.011

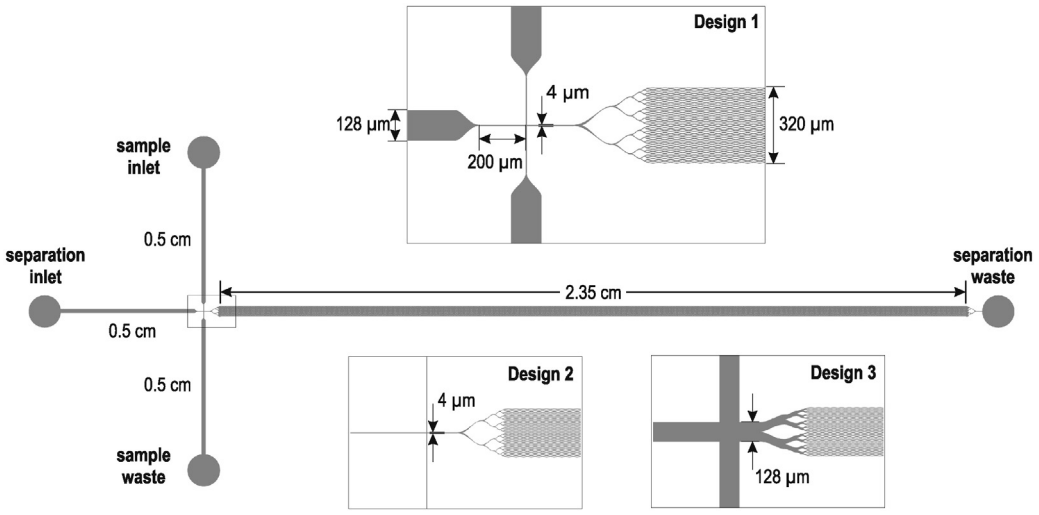

Fig. 1. Common design of the microchips. A cross layout is implemented. Injector/distributor structures with a total length of 310 μm (short version) or 620 μm (long version) are placed at 200 μm downstream of the injection cross. The main supply channel with 128 μm width is split into 32 channels in 5 branching steps. Design 1: Optimized distributor with reduced supply channels (from 128 μm to 4 μm upstream of the injection cross). Design 2: Optimized distributor with narrow supply channels (4 μm width). Design 3: Typical bifurcated distributor. Total column length and width are 2.29 cm and 320 μm, respectively. Collectors, which are the mirror image of the distributors, are placed at the end of the column. The total separation channel length is 3 cm wherein 28,823 pillar structures are placed. The chip drawing shows Design 1 as an example.

2. Experimental

2.1. Fabrication

Microchips were fabricated from fused silica with a simple 2-mask process as reported earlier [10]. The microchannels were dry etched in a 100 mm fused silica wafer with 500 μm thickness (Schott Lithotech) using an LPCVD poly-Si hard mask layer. Access holes were opened from the backside of the wafer via powder blasting using an in-house built setup. Next, a bare fused silica wafer was thermally bonded to close the channels. As a final step, the stack was diced and individual microchips were fabricated successfully (Figs. 2 and 3).

2.2. Microchip design and layout

A cross layout was implemented for the microchips with injector/distributor and collector structures placed at the beginning and at the end of the separation channel, respectively. Fig. 1 demonstrates the layout and dimensions. As mentioned in the introductory part, after theoretical optimization and experimental validation studies, the foil definition with 0° tip angle (see figure with Table 1) was selected as the only design reference for creating geometries. Like in our previous studies, a unit cell was defined as the building block of the separation column. The method for creating the foil geometry was described in detail in our earlier work [9].

Table 1
Geometrical parameters of the unit cell as a building block of the separation column. The design reference is the foil geometry, which is described as a 4th order polynomial with the maximum thickness at the center and 0° tip angle [9]. External porosity: 0.4, channel depth: 10 μm.

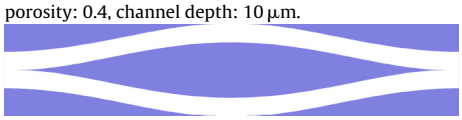

Unit cell length	50 μm
Unit cell width	10 μm
Pillar length	47 μm
Pillar width	6 μm
Minimum spacing	2 μm

Setting the unit cell dimensions as main parameters to be defined, the external porosity was defined as an additional parameter to generate the shape. Table 1 summarizes the geometrical properties of the unit cell (set parameters) and the pillar (generated parameters). The separation column was constructed by arraying these 32 by 458 times in lateral and longitudinal directions, respectively (Fig. 1).

The distributors were obtained by branching the main channel 5 times, yielding 32 channels at the end. As shown in Fig. 1, two types of distributors, yielding 3 different design cases, were implemented. The first type was the optimized distributor, which had a 4 μm wide inlet and distributed it to 32 channels with the same width. Therefore, the width of the main supply channels was reduced from 128 μm to 4 μm at one step with the curved profile shaped created by the foil definition at 200 μm upstream of the injection cross (Design 1). As an alternative, the width of the main supply channels was defined as 4 μm to fit with the inlet of the distributor without a reduction (Design 2). The second type was the typical bifurcated distributor (i.e. width of the branch is divided in two at each bifurcation point), which had a 128 μm wide inlet and distributed it to 32 channels with a width of 4 μm each (Design 3). All design cases were realized in two versions: short (total length of 310 μm) and long (total length of 620 μm).

The optimized distributor geometry was constructed using a modified unit cell definition similar to the one used for column design (0° foil). This time the pillar width was defined as an additional parameter to the unit cell dimensions instead of the external porosity and only the left half of the unit cell was drawn. This enabled controlling the channel widths. The inlet channel was branched into two channels with the same width as the inlet (4 μm). Based on this definition, the number of half unit cells was doubled and they were arrayed in lateral direction at every branching step. Also, their dimensions were scaled down to half of the previous step, while the inlet/outlet channel widths were fixed at 4 μm, which is the same inlet channel width of the column unit cell, for all steps. Fig. 2 shows a schematic drawing of the short version of the optimized distributor and a SEM picture of the fabricated structure. In total, 5 branching steps were performed to create the geometry, yielding 32 channels in the end. The resulting external porosity for optimized distributor design was 0.06, where it

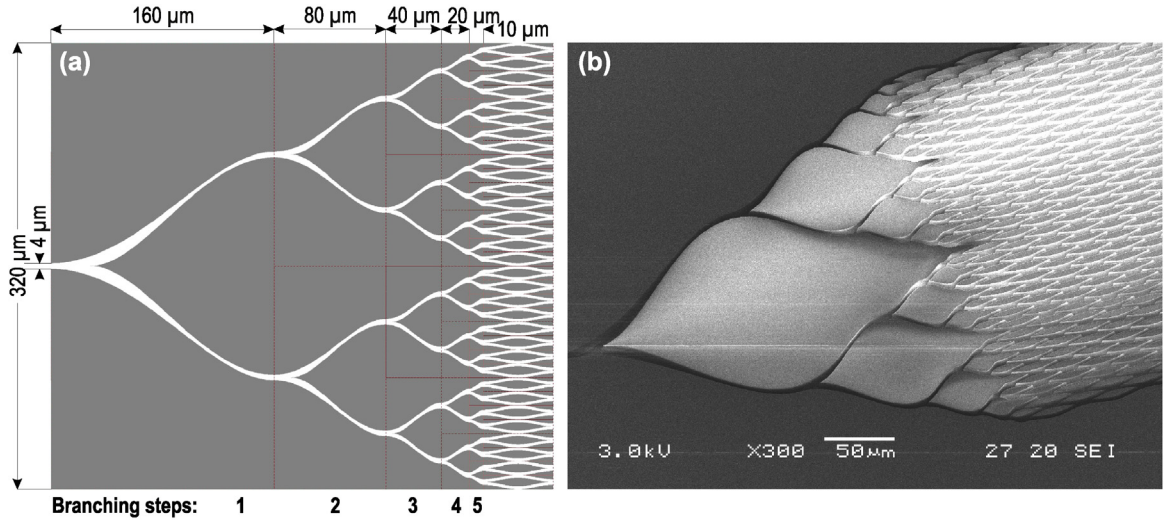

Fig. 2. Schematic representation (a) and SEM picture (b) of the fabricated optimized distributor design (short version). External porosity: 0.06.

was set at 0.4 for the separation column (the right most column in Fig. 2(a)).

Unlike the optimized distributor, the typical bifurcated geometry was constructed using the same definition as the column unit cell. In other words, the unit cell dimensions and the external porosity were defined. Half of the unit cell was drawn and the inlet channel was branched into two channels with half the width of the inlet. The number of half unit cells was doubled and they were arrayed in lateral direction at every branching step, while their dimensions were scaled down to half of the previous step (including the inlet/outlet channel widths). Therefore, the 128 μm wide supply channel was distributed to 32 channels with a width of 4 μm, which yields the same total width as the supply channel. Fig. 3 shows a schematic drawing of the short version of the typical bifurcated distributor and SEM picture of the fabricated structure.

2.3. Chemicals

Buffer solutions were prepared by dissolving phosphate buffer salt in DI water yielding 8.3 mM concentration. The prepared stock solutions were mixed with acetonitrile (ACN) in a 50:50 volumetric ratio. The Coumarin dyes (C440, C460, C480 and C540) were dissolved in HPLC-grade methanol in order to prepare sample stock solutions which will be diluted while dispensing into the reservoirs during the experiments. All the required chemicals were purchased from Sigma–Aldrich (Zwijndrecht, The Netherlands).

2.4. Chip coating procedure

Inner surfaces of the microchannels were coated with hydrophobic C18 monolayers in order to enable separation experiments under chromatographic retentive conditions. The same coating procedure as described earlier in detail [10] was applied. Methanol, dry toluene, coating solution (mixture of octadecyl trimethoxysilane and dry toluene with a 10:90 volumetric ratio), dry toluene and methanol were flushed through the microchannels, respectively.

2.5. Experimental procedure

Microchips were placed in a CNC-machined plastic (acetal copolymer) holder, which allows both interfacing the Nanoport connections for liquid pumping and having around 200 μL reservoirs sealed on top of each inlet/outlet opening. First, methanol

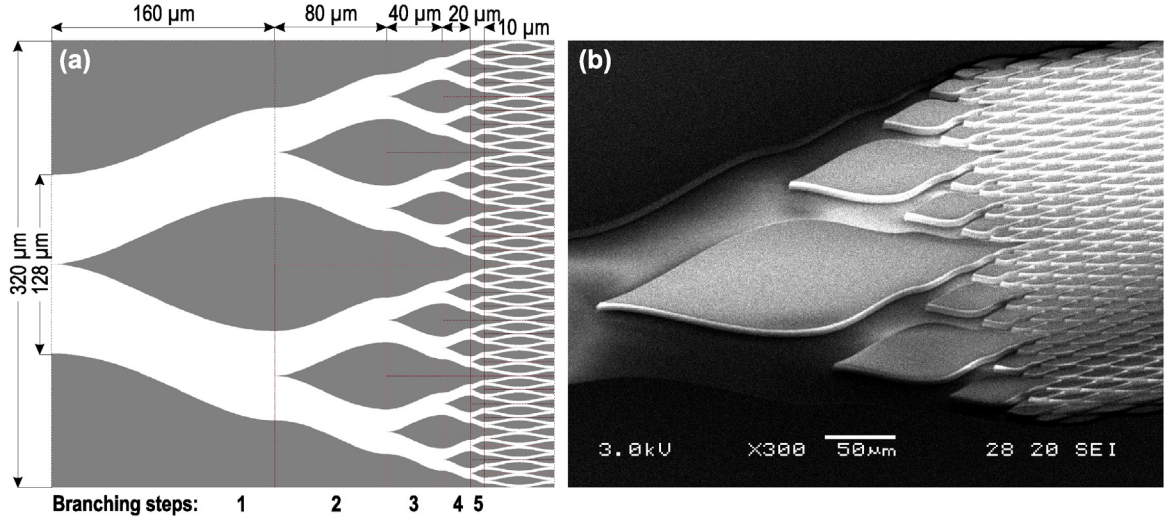

Fig. 3. Schematic representation (a) and SEM picture (b) of the fabricated typical bifurcated distributor design (short version). External porosity: 0.4.

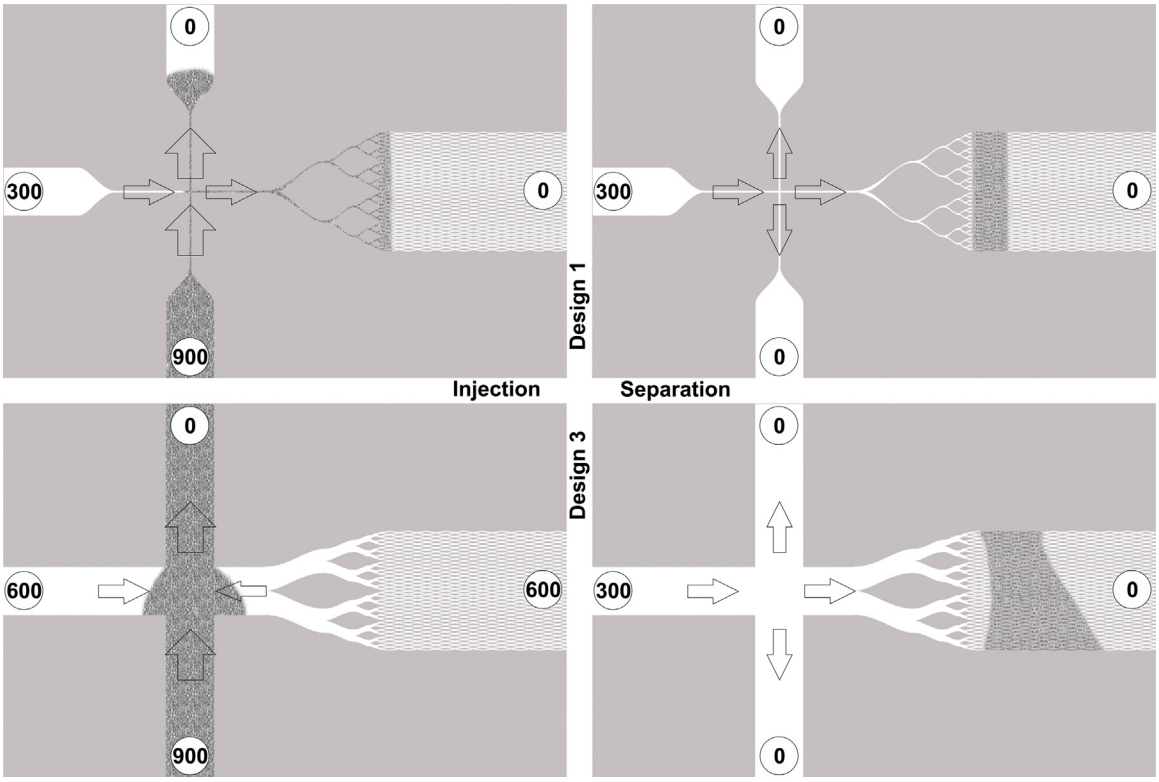

Fig. 4. Illustration of applied injection/separation voltages and corresponding sample profiles. Arrows represent the direction of flow in the corresponding arm. The same voltages were applied for Design 1 and 2 for injection experiments, therefore only Design 1 is included here. Pinching was applied during injection for Design 3.

was flushed for 10 min with a flow rate of 10 μL/min through the microchannels in order to wet the entire internal surface. Then phosphate buffer (pH 7.2, 8.3 mM concentration with 50:50 ACN volumetric composition) was pumped with a flow rate of 5 μL/min for 20 min. Switching between methanol and buffer streams was accomplished via a manual valve. Considering that the total internal volume of the microchips is around 50 nL, pumping 100 μL was enough to be sure that methanol was completely replaced with the buffer. After having the microchannels loaded, all the reservoirs were also filled with the buffer solution. Then 10 μL of 1 mM sample stock solution was dispensed into the sample inlet reservoir, which yielded a dilution to 5%. Subsequently, platinum wires, which serve as the electrodes, were immersed in the reservoirs. The voltages were applied with an 8 channel high voltage power supply (Labsmith HVS448-6000D, Mengel Engineering, Virum, Denmark). Injection was performed as described in the following sections. After the injection, the sample was directed into the separation channel by applying electric fields varying from 0.1 to 1 kV/cm.

2.6. Detection and data processing

Fluorescence spectroscopy was implemented as a detection method. A Leica DMI5000 M inverted microscope system (Leica Microsystems, Rijswijk, The Netherlands) which has an integrated motorized stage with electronic position control, was used for the experiments. As a light source a Leica EL6000 unit, equipped with a mercury short-arc lamp (Osram HXP-R120W/45C VIS, Leica Microsystems), was applied. Fluorescent emission from the sample was passed through a Leica filter cube: *D*, which consists of an excitation filter (band-pass 355–425 nm), a dichromatic mirror (455 nm) and a suppression filter (long-pass 470 nm). The experiments were monitored using a Leica DFC300 FX color camera attached to the microscope. Sample peaks were recorded at positions every 5 mm of the separation channel starting from the point of injection for mobility and plate height measurements. Resulting movie files were first decomposed into image sequences via VirtualDub (open source software), then analyzed and concentration profiles were plotted with ImageJ (open source). As a last step before the calculations, the plotted peaks were fitted as a Gaussian profile and the variances together with the residence times were directly extracted by using OriginPro 8 software (Origin Lab Corporation, USA).

3. Results and discussion

3.1. Injection analyses

Injection experiments were performed with uncoated devices as defined in the previous section. In order to evaluate the injection performance, snapshot images of the injected sample were taken at the moment that it entered the separation column (or left the distributor). Therefore these experiments consisted of two phases. First, the sample was guided to the injection cross for the typical bifurcated distributor (Design 3) or fed through the optimized distributors (Design 1 and 2) with the potentials shown in Fig. 4. Second, the sample was directed to the separation column by applying 300 V to the separation inlet reservoir while keeping the separation inlet, sample inlet and outlet reservoirs at 0 V (Fig. 4). This would cause a constant electric field of 300 V/cm through the entire separation channel for Design 3, since its cross-section is almost constant (the external porosity was kept at 0.4 everywhere). However, it was expected that the changes in the external porosities through the separation channel for Design 1 and 2 resulted with different values. The expected electric field values based on the channel electrical resistance calculations of around 400 V/cm and 60 V/cm through the injector and the separation channel, respectively for Design 1. Similarly, it was expected to be around 110 V/cm

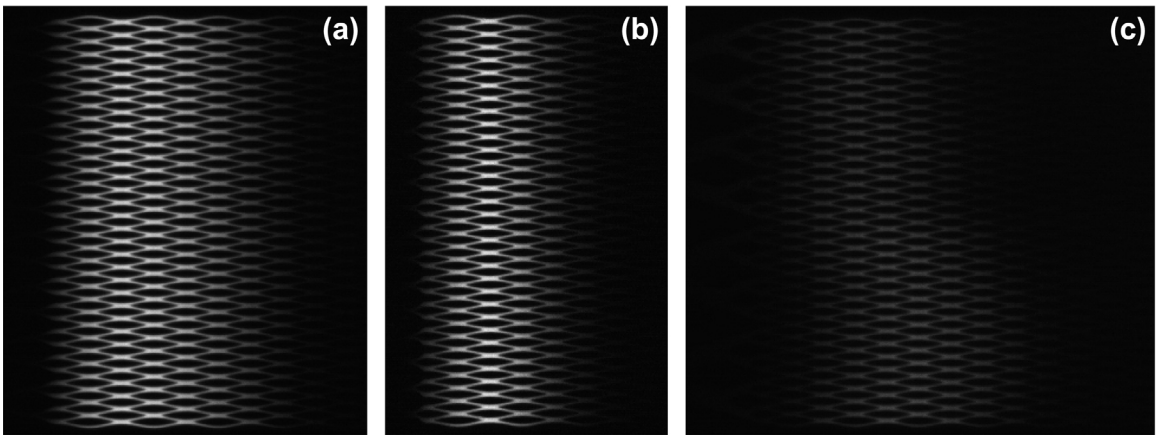

Fig. 5. Snapshot images of the injected sample at the distributor/separation column interface for the short versions of Design 1 (a), Design 2 (b) and Design 3 (c).

and 20 V/cm for the injector and the separation channel, respectively for Design 2.

Fig. 5 shows the snapshot images of the injected sample at the distributor/separation column interface for the short versions. For Design 1 and 2, Coumarin dye was fed for 0.8 and 0.6 s, respectively. Then the electric field was switched to the separation column. For Design 3, the sample stream was kept in the injection channel for 3 s to reach the equilibrium before switching the electric field. As seen in Fig. 5, Design 1 and 2 yielded almost constant width along the channel, while Design 3 resulted with a distorted shape. The images were processed and the base widths were calculated from the profile plots at every 50 μm in lateral direction along the channel. Fig. 6 represents the plot of the base width data. The calculated mean widths from experimental data for Design 1, 2 and 3 were 218, 165 and 255 μm, respectively. The deviation from the mean along the channel was only around 3–7 μm for optimized distributors (Design 1 and 2), while it was up to 50 μm for typical bifurcated distributor (Design 3).

The reason of the distorted shape for Design 3 was the initial profile created at the injection cross before the electric field switching. A more uniform distribution was obtained with the long version of the same distributor. Fig. 7 shows the initially created stream in its equilibrium shape and the snapshot image of the injected sample. The injection parameters, such as applied voltages and time periods, were the same as the short version.

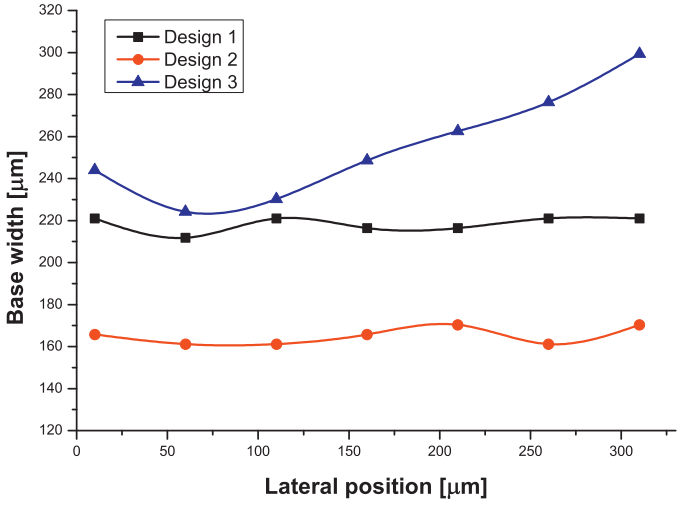

Fig. 6. Measured base widths of the injected sample shown in Fig. 5. The widths were measured at every 50 μm in lateral direction along the channel.

Since the external porosity and the separation channel length was the same for both versions, the same profiles were generated during injection (Fig. 7(a)). Applying the same electric field through the separation channel for switching enabled direct comparison of the sample profiles at the distributor/separation column interface. Although the variance in the width for the long version was decreased to around 19 μm, the mean base width was 348 μm. Hence, using the longer distributor caused a 36% increase in the base width of the sample (higher dispersion).

The shape of the initial profile can be changed by adjusting the pinching voltages during injection [11], which can be used for reducing the sample amount. However, the distorted shape cannot be avoided. Although reducing the sample amount could decrease the injected sample width, this would cause a decrease in the detected fluorescence intensity for the same initial sample concentrations. Lowered sensitivity causes loss of data during the detection and data processing and should be avoided. Moreover, the typical distributor design already caused a significant decrease in the detected signal. The short version of Design 3 caused 36% decrease in the amplitude of the intensity signal from injection cross (e.g. Fig. 7(a)) to distributor outlet (separation column inlet) (e.g. Fig. 7(b)). Comparing the two design alternatives, the long version of Design 3 yielded 43% lower amplitude in intensity signal when compared with the optimized designs (Design 1 and 2) for the same conditions (camera and exposure settings, initial sample concentration and volume, etc.). This is due to dispersion caused by molecular diffusion. On the other hand, optimized distributors cause no reduction in the fluorescence intensity at the injection phase while giving the ability of controlling the injected volume precisely by adjusting the duration of the feeding step. Fig. 8 illustrates the snapshot images of the long version of Design 1 for consecutive time steps for 500 V/cm applied electric fields after feeding with the voltages illustrated in Fig. 4. This experiment proved that the sample volume can be adjusted precisely without any sacrifice in the compactness of the injected sample profile with the optimized designs.

3.2. Design characterization experiments

This set of experiments was performed with bare fused silica microchips without any surface treatment (i.e. no stationary phase), which ensures an operation in non-retentive conditions. The concentration profile of the fluorescent dye C480 was monitored as described in the previous section. The presence of this neutral dye at a low concentration of around 0.1 mM caused no disturbance in the electric field distribution in the channel. Consequently, the migration of the corresponding zone of this dye

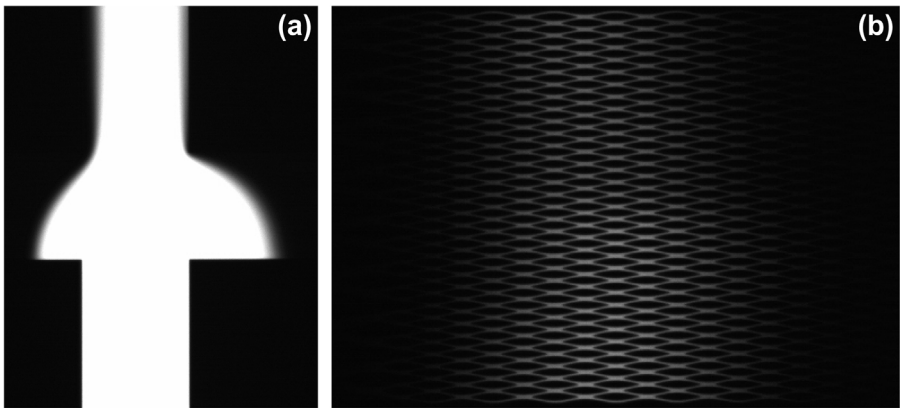

Fig. 7. Snapshot images of the sample stream in injection channel (a) and the injected sample at the distributor/separation column interface (b) for Design 3 (long version).

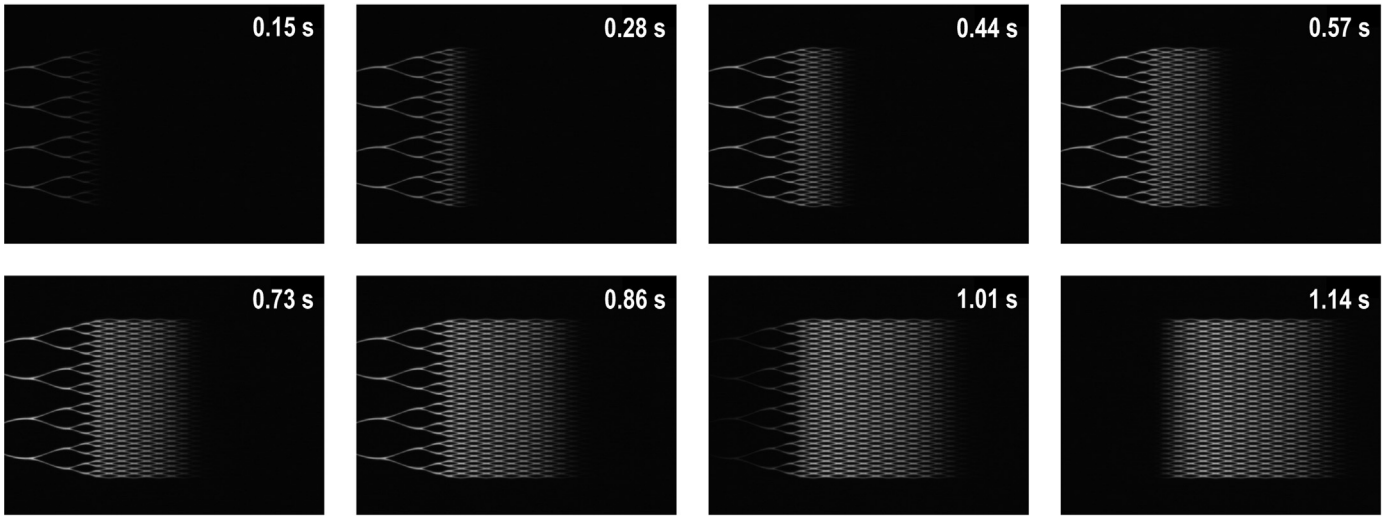

Fig. 8. Snapshot image series of Design 3 (long version) with time stamps for the injection experiment for controlling the injected sample volume. The last frame was captured immediately after injection was completed and the sample was guided to the separation column.

expresses the mobile phase velocity at the applied potentials. One of the key parameters to characterize an electrokinetic system is *mobility*. Therefore, the first parameter to be discussed as a performance measure for the different distributor geometries is the obtained velocity at a fixed voltage. Unlike its original definition, mobility is defined as the ratio of the obtained velocity to the applied voltage drop per unit centimeter of the separation channel, since the electric field is not uniformly distributed in axial direction of the channel. Fig. 9 shows the variation of the mobile phase velocity with respect to the applied voltage drop per unit cm of the separation channel. The relationship between these two parameters was linear, as expected. For a voltage drop of 800 V/cm, the measured mobile phase velocities were 0.71, 0.34, 1.11 and 1.44 mm/s for Design 1, Design 2, Design 3 and an empty channel without a separation column, respectively. Higher voltage drops caused instabilities because of joule heating for Design 1 and 2. However, these values of the electroosmotic flow (EOF) velocity, generated without surface treatment of the inner walls of the fused silica channels, are high enough for performing CEC experiments.

Being optimized for minimizing the change in the total cross sectional area in lateral direction, Design 3 caused 24% decrease in mobility when compared to an empty channel. However, employing a sharp decrease in external porosity (from 0.4 to 0.06) resulted with much higher voltage drops, hence a significant loss in the obtained linear velocities: Design 1 and 2 yielded 56% and 78% decrease, respectively, compared to an empty channel. Therefore,

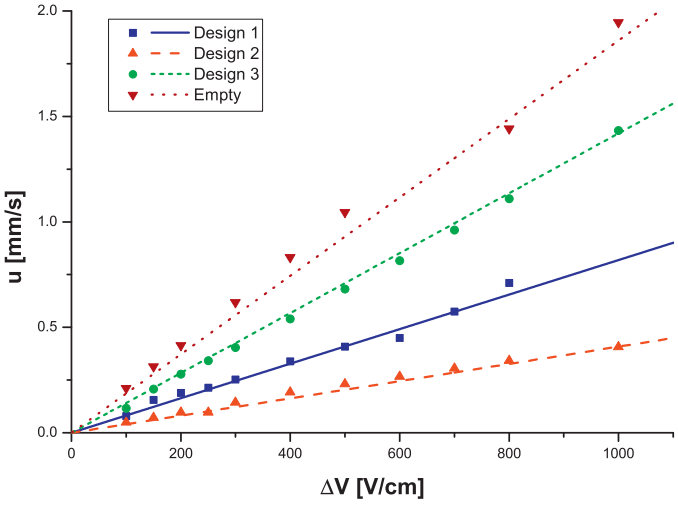

Fig. 9. Variation of the mobile phase velocity with the applied voltage drop per unit cm. A linear curve fit intercepting at (0,0) was implemented. Measured values of the electroosmotic mobility, which is the slope of the fitted curves, are 8.19E−9 m^2/V s for Design 1, 4.08E−9 m^2/V s for Design 2, 1.42E−8 m^2/Vs for Design 3 and 1.86E−8 m^2/Vs for the channel without column.

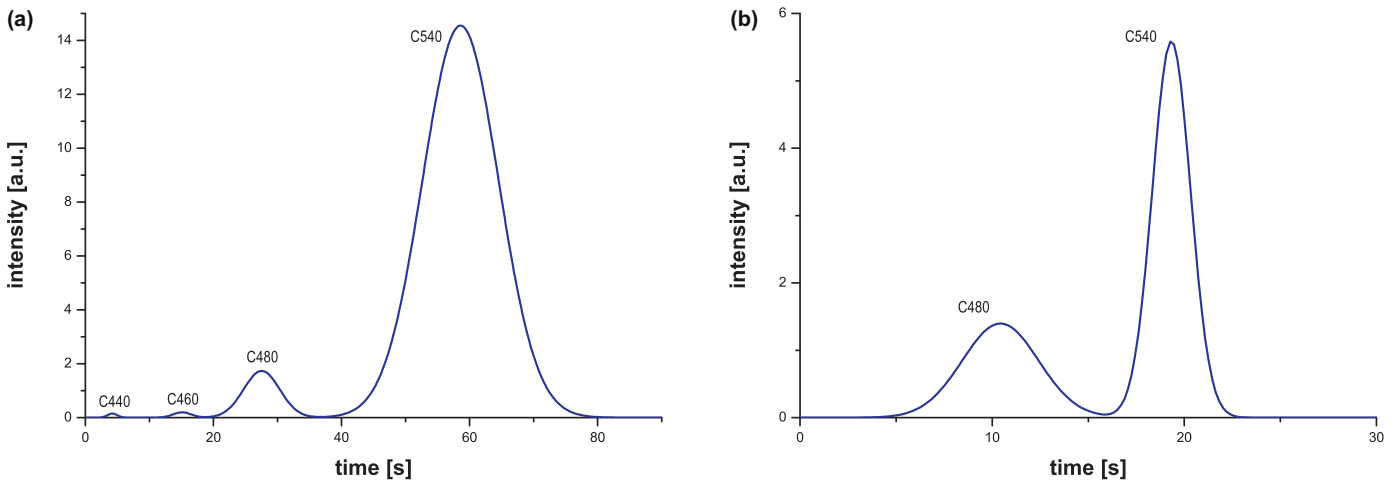

Fig. 10. 4 Coumarin dyes (C440, C460, C480 and C540) separated at 500 V/cm with Design 2 (a) and Design 3 (b). L_{sep} = 1 mm (Design 2) and 5 mm (Design 3). Stationary phase: octadecyl trimethoxysilane, mobile phase: phosphate buffer (pH 7.2 and 8.3 mM concentration with 50:50 ACN volumetric composition). Horizontal axis represents elapsed time after injection.

limiting the length of the narrowed (4 μm wide) main channel arms to 200 μm (Design 1) instead of deploying to full length (0.5 cm long, Design 2) produced twice as high velocities. Please note that the reduction in mobility is not only caused by the distributor and collector structures but also by the separation column placed in between, which has an external porosity of 0.4.

Extending the characterization studies and for determining the optimum working range of the microchips, band broadening was also studied by generating Van Deemter plots. The same column was coupled with all injector/distributor designs and the plate height calculations were performed for the respective measurement points inside the column. Therefore, it was expected to have no difference in A-, B- and C-terms of the fitted equations. Since the design of the pillars are the same as our previous work but the scale was smaller in this case, reduced parameters are discussed for enabling a direct comparison for the reader. For reduced parameters, A-term was missing for Design 1 and 2, where it was 0.1 for Design 3. Although this value is negligible, it could be the result of broadening of the sample during the injection, which was eliminated with the new designs as shown in previous sections. As expected, B-term was 2 and C-term was missing for all design cases. These findings showed a good agreement with our previous work. Plate heights as low as 1 μm were reached for non-retained species experiments.

In order to check the reliability of the measurements, the monitored velocities at different points in the separation channels were compared. The variances in the measured values were always within a 2% window, which proves the reliability of the data.

3.3. Separation experiments

With the aim of representing the potential of the optimized distributor design, separation experiments of 4 Coumarin dyes (C440, C460, C480 and C540) were performed with Design 2 and 3 at 500 V/cm voltage drop. This was the optimum working point for both designs as was concluded from the plate height graphs and/or separation performance at different potentials. The stock solutions at 1 mM concentration were mixed with the same volumetric ratio to prepare the dye mixture to be separated. Applying the same injection procedure as explained before, 50 μM initial concentration was obtained for each dye. Fig. 10 illustrates the separated 4 bands: C440, C460, C480 and C540. For Design 2, separation of all dyes was achieved at 1 mm downstream of the inlet of the separation column in less than 80 s with baseline resolution. For Design 3, only the signals of C480 and C540 could be detected with the same exposure conditions. The signals of C440 and C460 were lost after the first few hundreds of micrometers of the separation column after the point of injection. The samples were detected at 5 mm downstream. Although the analysis time was less than 30 s for Design 3, the sensitivity was much lower.

4. Concluding remarks

Application and experimental validation of the previously proposed foil definition in the design of injector/distributor structures for solid microfabricated column structures for CEC was presented. The effect of the optimized distributor designs on the injection performance in terms of the compactness of the injected sample was evaluated and the optimized designs yielded flat sample profiles. The proposed design approach enabled a precise control of the injected sample volume by means of adjusting the duration of the injection/feeding operation without sacrificing the compactness. More specifically, 165 and 218 μm base widths were obtained for 0.6 and 0.8 s of feeding, respectively. This revealed the linear relationship between the duration of the injection and the delivered sample amount.

One possible drawback of such design would be the high loss of the velocity arising from very low external porosities. Hence the analysis time would increase. However, the increased compactness of the injected plug enables separations in shorter separation lengths, which also decreases the analysis time.

In addition to the possibility of shorter channels, the discussed architecture would also allow a T-shaped chip layout instead of a cross arrangement [12]. The injection cross is not needed anymore since the injection is performed as a feeding operation. In other words, only one sample feeding arm would be necessary. Therefore, more compact microchips with less device area would be possible using such optimized distributor structures. For example, the width of the microchip used in this study could be lowered by a factor of 2 (from 1 to 0.5 cm) by avoiding one of the injection channel arms.

Acknowledgements

This work was financially supported by IWT-Flanders within the NextChrom project.

References

[1] B. He, N. Tait, F. Regnier, Anal. Chem. 70 (1998) 3790.
[2] X. Zhang, F.E. Regnier, J. Chromatogr. A 869 (2000) 319.
[3] B.E. Slentz, N.A. Penner, F. Regnier, J. Sep. Sci. 25 (2002) 1011.
[4] O. Gustafsson, K.B. Mogensen, J.P. Kutter, Electrophoresis 29 (2008) 3145.
[5] K.B. Mogensen, F. Eriksson, O. Gustafsson, R.P.H. Nikolajsen, J.P. Kutter, Electrophoresis 25 (2004) 3788.
[6] J. Vangelooven, W. De Malsche, J. De Beeck, H. Eghbali, H. Gardeniers, G. Desmet, Lab Chip 10 (2010) 349.
[7] J. Vangelooven, S. Schlautman, F. Detobel, H. Gardeniers, G. Desmet, Anal. Chem. 83 (2011) 467.
[8] W. De Malsche, J. Op De Beeck, S. De Bruyne, H. Gardeniers, G. Desmet, Anal. Chem. 84 (2012) 1214.
[9] S. Sukas, G. Desmet, H.J.G.E. Gardeniers, Electrophoresis 31 (2010) 3681.
[10] S. Sukas, W. De Malsche, G. Desmet, H.J. Gardeniers, Anal. Chem. 84 (2012) 9996.
[11] S.V. Ermakov, S.C. Jacobson, J.M. Ramsey, Anal. Chem. 72 (2000) 3512.
[12] C. Tsai, R. Yang, C. Tai, L. Fu, Electrophoresis 26 (2005) 674.